

## Dissipative Localized States with Shieldlike Phase Structure

Marcel G. Clerc,<sup>1</sup> Saliya Coulibaly,<sup>2</sup> Mónica A. Garcia-Ñustes,<sup>1</sup> and Yair Zúrate<sup>1</sup>

<sup>1</sup>*Departamento de Física, Facultad de Ciencias Físicas y Matemáticas, Universidad de Chile, Casilla 487-3, Santiago, Chile*

<sup>2</sup>*Laboratoire de Physique des Lasers, Atomes et Molécules, CNRS UMR 8523, Université des Sciences et Technologies de Lille–59655 Villeneuve d'Ascq Cedex, France, EU*

(Received 30 June 2011; published 14 December 2011)

A novel type of parametrically excited dissipative solitons is unveiled. It differs from the well-known solitons with constant phase by an intrinsically dynamical evolving shell-type phase front. Analytical and numerical characterizations are proposed, displaying quite a good agreement. In one spatial dimension, the system shows three types of stationary solitons with shell-like structure whereas in two spatial dimensions it displays only one, characterized by a  $\pi$ -phase jump far from the soliton position.

DOI: 10.1103/PhysRevLett.107.254102

PACS numbers: 05.45.Yv, 89.75.Kd

Macroscopic systems maintained out of equilibrium are characterized by the possibility of the emergence of particle-type solutions or localized states. These states have been observed in different fields such as magnetic materials, liquid crystals, gas discharge, chemical reactions, fluids, granular media, and nonlinear optics media, among others (see the reviews [1–3], and references therein). Although these states are spatially extended, they exhibit properties typically associated with particle-like states. Consequently, one can characterize them with a family of continuous parameters such as position, amplitude, and width. For time-reversible systems where injection and dissipation of energy can be viewed as perturbations—quasireversible systems [4]—the prototype model that exhibits localized states is the parametrically driven damped nonlinear Schrödinger equation [5]. This model has been derived in several contexts to describe the appearance of patterns and localized structures, such as vertically vibrated Newtonian fluid layers [6], nonlinear lattices [7], optical fibers [8], Kerr type optical parametric oscillators [9], easy-plane ferromagnetic materials exposed to an oscillatory magnetic field [10], and a parametrically driven damped chain of pendula [11]. One of the greatest benefits of this model is to present analytical solutions for localized states characterized by a constant phase and a bell-like shape for the amplitude [10].

In this Letter, we show that localized states of quasireversible parametric systems present an unexpectedly rich phase front dynamics. More precisely, the stationary localized states have a shell-type structure in the phase, for a large range of parameters. These stable structures are of three types. We term these solutions phase shielding solitons. Using the asymptotic amplitude equation, valid far from the position of the localized states, we determine analytically the shape of phase fronts and its dynamics. This dynamics is characterized by the juxtaposition of two forces, one due to relative stability between the phases and the other related to spatial variations of the tail of the dissipative soliton. As a result of this force balance, these

localized states exhibit a phase structure that shields the soliton. Numerical simulations show quite good agreement with our analytical predictions.

The envelope of an oscillation for extended conservative systems in the presence of small energy injection through a parameter modulation and energy dissipation—via damping phenomena—is described by the parametrically driven damped nonlinear Schrödinger equation

$$\partial_t \psi = -i\nu\psi - i|\psi|^2\psi - i\partial_{xx}\psi - \mu\psi + \gamma\bar{\psi}, \quad (1)$$

where the envelope  $\psi(x, t)$  is a one-dimensional complex field,  $\bar{\psi}$  stands for the complex conjugate of  $\psi$ , and  $\{x, t\}$  describe, respectively, the spatial and temporal coordinates. The detuning parameter is  $\nu$ , which is proportional to the difference between half of the forcing frequency and the natural frequency of the oscillator field.  $\mu$  is the damping parameter, and  $\gamma$  stands for the forcing amplitude of the parametric forcing. The higher-order terms in Eq. (1) are ruled out by a scaling analysis, since  $\mu \ll 1$ ,  $\nu \sim \mu \sim \gamma$ ,  $|\psi| \sim \mu^{1/2}$ ,  $\partial_x \sim \mu^{1/2}$ , and  $\partial_t \sim \mu^{1/2}$ .

Introducing the following change of variables  $\psi = R(x, t)e^{i\varphi(x, t)}$  in Eq. (1), the model reads

$$\partial_t R = 2\partial_x R \partial_x \varphi + R \partial_{xx} \varphi - \mu R + \gamma R \cos(2\varphi), \quad (2)$$

$$\partial_t \varphi = -\nu - R^2 - \frac{\partial_{xx} R}{R} + (\partial_x \varphi)^2 - \gamma \sin(2\varphi), \quad (3)$$

where  $R$  and  $\varphi$  stand for the amplitude and phase of  $\psi$ , respectively. The previous set of equations in the region of parameters  $-\nu - \sqrt{\gamma^2 - \mu^2} \geq 0$ , exhibit stationary dissipative solitons of the form  $R_s(x, x_0) = \sqrt{2\delta} \operatorname{sech}(\sqrt{\delta}[x - x_0])$  and  $\varphi_s = \arccos(\mu/\gamma)/2$  with  $\delta \equiv -\nu + \sqrt{\gamma^2 - \mu^2}$  [10] [see Fig. 1(a)]. Hence, the localized states are defined as having a bell shape in the modulus and a constant phase. However, when we try to observe the previous solution, numerical simulations show that an unexpected and rich phase dynamics arises. Such dynamics initially establishes a bell shape in the modulus

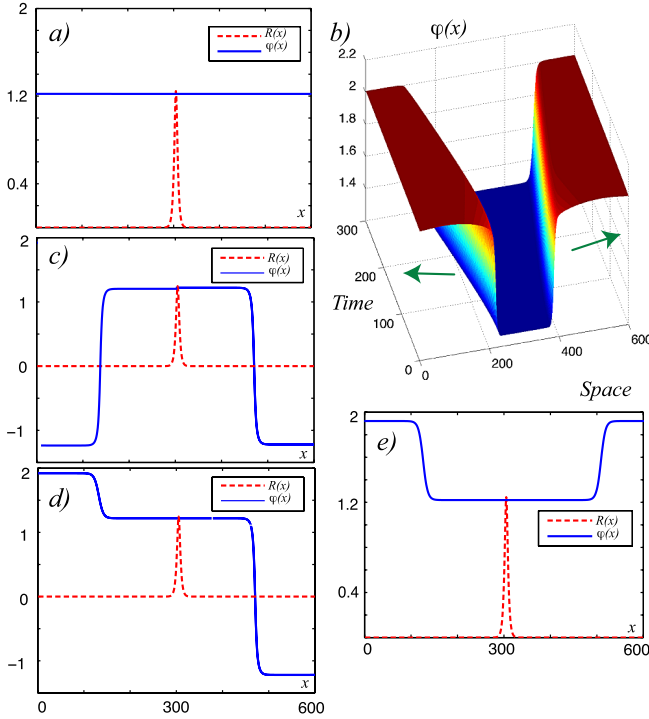


FIG. 1 (color online). Solitons in the parametrically driven damped nonlinear Schrödinger equation: (a) soliton with constant phase; (b) space-time diagram for the phase  $\varphi(x, t)$  of Eq. (1) with  $\gamma = 0.123$ ,  $\nu = -0.093$ , and  $\mu = 0.100$ ; (c), (d), and (e) solitons with phase shell-like structure obtained numerically from Eq. (1) for  $\gamma = 0.083$ ,  $\nu = -0.063$ , and  $\mu = 0.058$ .

of the amplitude. Then, a constant phase appears around the position of the localized state. At a latter stage, after some intricate transients, a pair of fronts that connect different phase equilibrium emerge. These equilibria are characterized by  $\cos(2\varphi_0) = \mu/\gamma$ . Finally, a rather slow dynamics of phase front propagation is established, which ends with the formation of a pair of stationary fronts that connect steady states. Figure 1(b) illustrates the above described time evolution of phase dynamics. The system has four phase equilibria in the range from  $-\pi$  to  $\pi$ . Therefore, the stable dissipative solitons have three types of shell-like phase structures. Figures 1(c)–1(e) outline these solutions. Because of the fact that the function  $\cos(2\varphi)$  has period  $\pi$ , the phase difference at the ends of the dissipative soliton can be zero or  $\pi$  (cf. Fig. 1). Thus, this last localized state is characterized by a phase difference given by zero around the core and  $\pi$  at the ends. It is important to mention that dissipative solitons represented in Figs. 1(a), 1(c), and 1(e), are homoclinic orbits for the spatial system in polar representation  $\{R, \varphi\}$ . However, the dissipative soliton shown in Fig. 1(d) corresponds to a heteroclinic solution. In Cartesian representation  $\{\text{Re}(A), \text{Im}(A)\}$  all these solutions correspond to homoclinic orbits.

For the purpose of understanding and capturing the wealth of these phase front solutions, let us consider

Eq. (1) in a semi-infinite domain, with zero flux boundary conditions. The system can exhibit a dissipative soliton located at one edge, with the phase formed by a single front [see Fig. 2(a)]. In addition it is worth noting that these phase fronts emerge at a distance far from the core of the soliton, i.e., at a distance much larger than  $1/\sqrt{\delta}$ . Accordingly,  $R(x, x_0) \approx 2\sqrt{2\delta}e^{-\sqrt{\delta}(x-x_0)}$  for  $x - x_0 \gg 0$ , with  $x_0$  at the left edge of the region of interest. Together with Eq. (2) this approximation leads to the following Newton-type equation

$$\partial_{xx}\varphi = 2\sqrt{\delta}\partial_x\varphi + \mu - \gamma\cos(2\varphi). \quad (4)$$

This equation has heteroclinic solutions corresponding to phase fronts, which analytically are well described by

$$\varphi_F(x, x_f) \approx \arctan\left[\sqrt{\frac{\gamma \pm \mu}{\gamma \mp \mu}} \tanh\frac{\sqrt{\gamma^2 - \mu^2}(x - x_f)}{2\sqrt{\delta}}\right], \quad (5)$$

where  $x_f$  accounts for the position of phase front, i.e., the point at which the spatial derivative of the phase front has its global maximum. Thus, the phase front solutions are parametrized by a continuous parameter  $x_f$ . Figure 2 shows the numerically computed phase fronts, which present a difference of 1% with respect to expression (5). Notice that if one considers the first correction to the previous equation  $\varphi \approx \varphi_F + \partial_x\varphi_F/2\sqrt{\delta}$  this difference decreases to 0.8%.

As it can be also seen from Fig. 2(b), this front displays an unexpected dynamical behavior characterized by a non-uniform translation. To describe this dynamics, we promote the front position to a time-dependent function  $x_f(t)$ . Hence, using Eq. (3) and formula (5), we obtain

$$-\dot{x}_f\partial_x\varphi_F = -(\nu + \delta) - 8\delta e^{-2\sqrt{\delta}x} + (\partial_x\varphi_F)^2 - \gamma\sin(2\varphi_F), \quad (6)$$

where  $\dot{x}_f$  stands for the time derivative of  $x_f$ . Multiplying the above equation by  $\partial_z\varphi_F$  with  $z \equiv x - x_f$ , and introducing the following inner product  $\langle f|g \rangle \equiv \int fg dz$ , we obtain the following equation for the phase front after straightforward calculations,

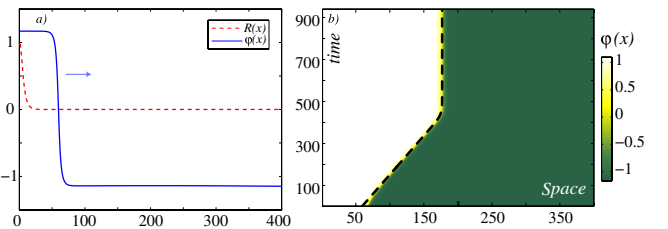


FIG. 2 (color online). Phase propagation: (a) phase front profile considering half of the dissipative soliton; (b) spatiotemporal diagram of phase front obtained from Eq. (1) by  $\gamma = 0.083$ ,  $\nu = -0.063$ , and  $\mu = 0.058$ . The dashed curve is the numerical solution obtained using Eq. (7).

$$\dot{x}_f = A + B e^{-2\sqrt{\delta}x_f}, \quad (7)$$

where

$$A \equiv \frac{\langle (\nu + \delta + \gamma \sin(2\varphi_F) - (\partial_z \varphi_F)^2) | \partial_z \varphi_F \rangle}{\langle \partial_z \varphi_F | \partial_z \varphi_F \rangle},$$

$$B \equiv 8\delta \frac{\langle e^{-2\sqrt{\delta}z} | \partial_z \varphi_F \rangle}{\langle \partial_z \varphi_F | \partial_z \varphi_F \rangle}$$

are real numbers, which can be either positive or negative depending on the shape of the phase front. For example, when one considers a front that increases monotonically with the spatial coordinate,  $A$  ( $B$ ) is a negative (positive) constant. The term proportional to  $A$  accounts for the constant speed at which the larger phase invades the smaller value. This speed can be understood as a consequence of the energy difference between these states. Hence, this term gives rise to phase fronts propagating towards the soliton position. Conversely, the term proportional to  $B$  accounts for the effect of spatial variation of the tail of the amplitude soliton, which induces a force that leads to phase fronts moving away from the localized state. Consequently, the superposition of these two opposing forces generates a stable equilibrium for the position of the phase front, which is consistent with the dynamics illustrated in the space-time diagram in Fig. 2. The dashed curve in Fig. 2(b) represents the solution obtained from Eq. (7), using the above formulas  $A$  and  $B$ . Modifying the parameters, we observe that as  $\gamma$  increases the equilibrium position is smaller; i.e., the shell-type structure surrounding the soliton decreases. Instead, as  $\nu$  increases the equilibrium position of the phase front also grows.

Considering now the soliton located at the center of the spatial region, a small disturbance on the system produces some complex transients on the phase dynamics, ending by the formation of a pair of fronts propagating in opposite directions away from the soliton core. The dynamics of these fronts differs from that of the single front by the inclusion of an interaction process which decays exponentially with the distance between the fronts. As the system displays two types of phase fronts monotonically increasing or decreasing, then the soliton exhibits three different types of shield structures in its phase, as shown in Fig. 1. Hence, the dissipative solitons in parametrically driven systems have a rich dynamics of phase fronts.

To understand the correspondence between the constant phase solitons and phase shielding solitons, we have performed a numerical linear stability analysis similar to the one made in Ref. [12], considering both the control parameters and size of the system  $L$ . When  $L$  is small enough the spectrum—set of eigenvalues associated with the linear stability analysis—is characterized by being centered on an axis parallel to the imaginary one [cf. Fig. 3(b)], where every single eigenvalue has negative real part. Increasing  $L$  the set of eigenvalues begin to collide creating a curve of eigenvalues (a continuum). For a critical value of  $L$  this

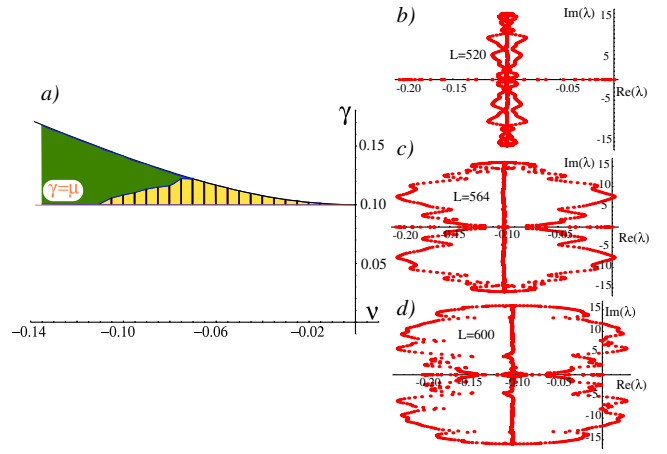


FIG. 3 (color online). Stability of solitons: (a) schematic representation of bifurcation diagram in the  $\gamma - \nu$  space for  $\mu = 0.050$ , the shaded region corresponds to the phase shielding soliton region, and the striped area is the region of soliton with constant phase. (b), (c), and (d) are the spectra of the soliton with constant phase before (system size  $L = 520$ ), during ( $L = 564$ ), and after ( $L = 600$ ) the bifurcation, respectively, for  $\gamma = 0.263$ ,  $\mu = 0.050$ , and  $\nu = -0.083$ .

curve collides with the imaginary axis at a nonzero frequency [cf. Fig. 3(c)]. Therefore the system exhibits an Andronov-Hopf bifurcation. Figure 3 outlines the spectrum before, during, and after the bifurcation.

From previous numerical analysis, one can infer that the soliton with homogeneous phase is unstable, over a wide parameter region, for sufficiently large values of  $L$ . In short, there exists a critical value of  $L$  for which the soliton with constant phase is unstable to small perturbations in phase and amplitude. Because of the analytical complexity of this analysis, we have only determined numerically this critical value. For a system size smaller than the critical one, we observe that for parameters  $0 < \gamma - \mu \ll 1$ , the soliton with constant phase is stable. Increasing the forcing amplitude  $\gamma$ , the soliton becomes unstable by an Andronov-Hopf bifurcation similar to the one shown in Fig. 3. This figure illustrates the region in parameter space where this solution is stable and unstable. In the shaded region in Fig. 3, we found stable phase shielding solitons.

To study the robustness of the phase dynamics around the soliton, we consider the two-dimensional spatial extension of Eq. (1), that is, the  $\partial_{xx}$  operator is replaced by a two-dimensional Laplacian operator  $\nabla^2 = \partial_{xx} + \partial_{yy}$ . It is well known that this equation has soliton type solutions with a constant phase [13], which are the natural extensions of the one-dimensional case. However, an analytical expression for these solutions is unknown. Considering a similar parameter region of phase shielding solitons in one dimension, we observe a rich phase fronts dynamics in two dimensions. If one slightly perturbs the soliton, after some complex transient in the phase dynamics we observe the appearance of a circular phase front that spreads slowly.

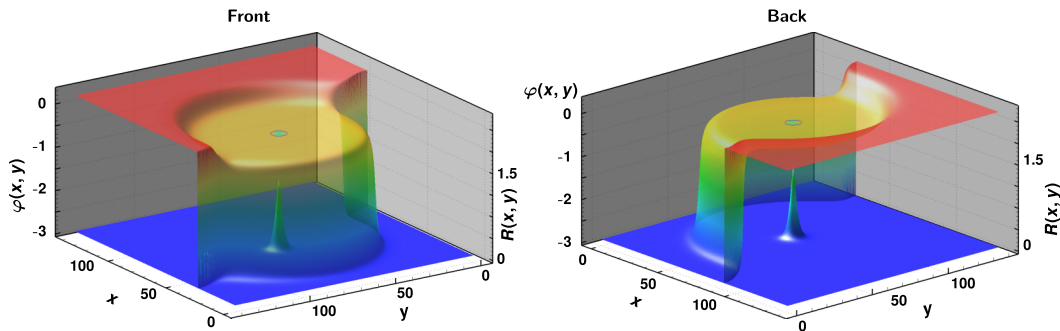


FIG. 4 (color online). Front and back view of a stationary phase shielding soliton observed in two dimensions for the parametrically driven damped nonlinear Schrödinger equation with  $\gamma = 0.140$ ,  $\nu = -0.068$ , and  $\mu = 0.125$ . The phase and amplitude field are represented simultaneously. The colored shadow renders the phase shell-like structure  $[\varphi(x, y)]$  that surrounds the amplitude soliton localized at the center  $[R(x, y)]$ .

For later times, the front becomes asymmetric, giving rise to another front. Finally, the two fronts become stationary, creating a shieldlike structure around the soliton. Figure 4 shows the stationary phase structure observed numerically in a two-dimensional system. It is important to note that we only see phase shielding structure as a state of equilibrium for dissipative soliton in a large system size. The two-dimensional solution is characterized by being composed of all the solutions found in one dimension. Indeed, if one performs different cuts containing the center (soliton position), one can recognize the observed solutions in one dimension (see Fig. 1). A surprising property of the shell-like structure observed is that if one calculates the phase change on a path that connects two opposite points with respect to the position of the soliton ( $\int_{\Gamma} \vec{\nabla} \varphi d\vec{s}$ ) within the region close to the position of the soliton one finds that this is zero. Nevertheless, if one takes this type of path far away from the soliton position, one finds  $\int_{\Gamma} \vec{\nabla} \varphi d\vec{s} = \pm \pi$ .

In conclusion, localized structures in parametrically forced systems have a rich and unexpected phase dynamics, creating novel types of localized states. We expect that phase shielding solitons could be observed experimentally in simple coupled forced oscillators, such as vertically driven fluid layers in narrow cells, optical parametrical oscillators, driven magnetic media, and a chain of coupled oscillators.

Shell-like phase structure must play a significant role in soliton interaction, since bound states of two solitons show a complex phase structure [14]. Experimental observations show an intricate temporal dynamics of dissipative solitons [15] which cannot be explained from uniform phase solitons. Work in this direction is in progress.

The authors thank C. Falcón for fruitful discussions. The authors acknowledge financial support by the ANR-CONICYT 39, “Colors.” M.G.C. and M.A.G-N. are thankful for the financial support of FONDECYT

Projects No. 1090045 and No. 3110024, respectively. M. G. C. also acknowledges ACT Project No. 127.

- 
- [1] *Localized States in Physics: Solitons and Patterns*, edited by O. Descalzi, M. Clerc, S. Residori, and G. Assanto (Springer, New York, 2010).
  - [2] H. G. Purwins, H. U. Bodeker, and Sh. Amiranashvili, *Adv. Phys.* **59**, 485 (2010).
  - [3] T. Ackemann, W. J. Firth, and G. L. Oppo, *Adv. At. Mol. Opt. Phys.* **57**, 323 (2009).
  - [4] M. Clerc, P. Coulet, and E. Tirapegui, *Phys. Rev. Lett.* **83**, 3820 (1999); *Int. J. Bifurcation Chaos Appl. Sci. Eng.* **11**, 591 (2001); *Opt. Commun.* **167**, 159 (1999); *Phys. Lett. A* **287**, 198 (2001); *Prog. Theor. Phys. Suppl.* **139**, 337 (2000).
  - [5] I. V. Barashenkov and E. V. Zemlyanaya, *Phys. Rev. Lett.* **83**, 2568 (1999).
  - [6] J. W. Miles, *J. Fluid Mech.* **148**, 451 (1984); W. Zhang and J. Viñals, *Phys. Rev. Lett.* **74**, 690 (1995); X. Wang and R. Wei, *Phys. Rev. E* **57**, 2405 (1998); M. G. Clerc *et al.*, *Phil. Trans. R. Soc. A* **367**, 3213 (2009).
  - [7] B. Denardo *et al.*, *Phys. Rev. Lett.* **68**, 1730 (1992).
  - [8] J. N. Kutz *et al.*, *Opt. Lett.* **18**, 802 (1993).
  - [9] S. Longhi, *Phys. Rev. E* **53**, 5520 (1996).
  - [10] I. V. Barashenkov, M. M. Bogdan, and V. I. Korobov, *Europhys. Lett.* **15**, 113 (1991); M. G. Clerc, S. Coulibaly, and D. Laroze, *Physica (Amsterdam)* **239D**, 72 (2010).
  - [11] N. V. Alexeeva, I. V. Barashenkov, and G. P. Tsironis, *Phys. Rev. Lett.* **84**, 3053 (2000).
  - [12] N. V. Alexeeva, I. V. Barashenkov, and D. E. Pelinovsky, *Nonlinearity* **12**, 103 (1999).
  - [13] I. V. Barashenkov, N. V. Alexeeva, and E. V. Zemlyanaya, *Phys. Rev. Lett.* **89**, 104101 (2002).
  - [14] I. V. Barashenkov and E. V. Zemlyanaya, *Phys. Rev. E* **83**, 056610 (2011); E. Kenig *et al.*, *Phys. Rev. E* **80**, 046202 (2009).
  - [15] W. Wei *et al.*, *Phys. Lett. A* **219**, 74 (1996).